

Diffusion Properties of Dye Molecules in Nanoporous TiO₂ Networks

M. Dürr,* A. Schmid, M. Obermaier, A. Yasuda, and G. Nelles

Materials Science Laboratory, Sony Deutschland GmbH, 70327 Stuttgart, Germany

Received: December 21, 2004; In Final Form: March 3, 2005

The adsorption of ruthenium-dye molecules out of ethanol solution onto TiO₂ particles of nanoporous TiO₂ films was used to study the molecules' diffusion through these layers by means of optical absorption spectrometry. Dependent on pore size, porosity, and particle size, effective diffusion constants as low as $D_{\text{eff}} = 4 \times 10^{-9} \text{ cm}^2/\text{s}$ were deduced from the uptake curves by applying a simple model for combined diffusion and adsorption. These diffusion constants for diffusion through the nanoporous network are up to 3 orders of magnitude lower than in bulk ethanol and are discussed with respect to the properties of the nanoporous material.

Porous wide band-gap semiconductor materials, especially TiO₂, are of importance in a variety of photoelectrochemical applications.^{1–3} As one example, sensitization of nanoporous TiO₂ with molecules capable of absorbing light in the visible range of the solar spectrum has led to the development of an effective photovoltaic device, the so-called dye-sensitized solar cell (DSSC).⁴ Regarded as a low-cost alternative to conventional bulk-semiconductor devices, much effort has been put on the investigation and improvement of the cell as such, as well as many of the subsystems of the complex device have become an own field of research. However, diffusion processes in the porous network of DSSCs have been studied in greater detail only recently^{5,6} and no quantitative investigation of the diffusion processes of dye molecules through the nanoporous network have been reported so far. Because this is the most common way to adsorb dye molecules out of solution on the porous TiO₂, the process is of importance for future mass production of the DSSC. But also from a fundamental point of view the diffusion of molecules with dimensions in a comparable order of magnitude as the pores of the network seems to be interesting. Kärger and co-workers measured self-diffusion of azobenzene in porous glass by means of NMR but the results were strongly influenced by chemically reactive surface sites.⁷ To eliminate such interference by chemical trapping and detrapping, Dozier et al. passivated the surface when measuring self-diffusion of azobenzene in porous Vycor glass by means of forced Rayleigh scattering.⁸ By this they found a strong decrease of the effective diffusion constant in the porous network compared to diffusion in the bare solvent. Further investigations on the diffusion of polymers in porous Vycor glass include the dependence on molecule size⁹ and its modeling by reconstructing the porous media.¹⁰ Only little experimental effort has been reported so far on the influence of the parameters of the nanoporous material on the diffusion constants.

In this contribution, we make use of the diffusion limitations to the adsorption of dye molecules on TiO₂ to investigate their diffusion properties in nanoporous networks in more detail. We report on the diffusion properties of *cis*-bis(isothiocyanato)-bis-(2,2'-bipyridine-4,4'-dicarboxylato)ruthenium(II) bis(tetrabutylammonium), in short red dye, through nanoporous TiO₂ of

TABLE 1: Characteristic Data on the Porous Films as Well as Diffusion Constants Obtained for Red Dye in Those Films

	porosity [%]	pore diam [nm]	particle diam [nm]	D_{eff} [$10^{-9} \text{ cm}^2/\text{s}$]	D_0 [$10^{-9} \text{ cm}^2/\text{s}$]
(1)	69	22	20	7.0	10
(2)	63	18	20	4.3	6.8
(3)	63	13	14	3.7	5.9

variable but well-defined porosity, particle size and pore size distribution. A simple model is shown to be capable of reproducing the uptake curves obtained by means of optical absorption spectrometry (UV–vis spectrometry) and hence the effective diffusion constants have been obtained. Because the reactive TiO₂ surface is passivated by the diffusing dye molecules themselves, reactive trapping can be excluded and comparison with diffusion in pure ethanol shows the dramatic effect of the geometry of the porous network on the diffusion process. The effective diffusion constant is found to be reduced by up to 3 orders of magnitude in the porous layers. The influence of pore size is found to be an important parameter, but particle size, and with this the number and size of the interconnections between the pores, also play a decisive role for changing the diffusivity in the porous network.

The nanoporous TiO₂ layers used in the experiments consist of anatase TiO₂ particles synthesized by means of thermal hydrolysis, which allows for different particle sizes as a function of reaction temperature.¹¹ Films of different thickness have been fabricated by screen printing terpeneol based paste through different meshes on glass substrates. The porosity of the layers has been adjusted by the amount of organic contents in the paste. Sintering such films at 450 °C results in burning all organic binders and ensures good contact between the single particles. The porosity of the films was determined by means of nitrogen adsorption; Barrett–Joyner–Halenda (BJH) analysis of the nitrogen adsorption and desorption isotherms reveals the mean pore size and gives a measure of the pore openings, respectively. The data are summarized in Table 1 for the porous materials used in this investigation and are labeled (1)–(3) in the following. Examples of the BJH analysis are shown in Figure 1 together with scanning electron micrographs of the respective porous layers. For measurements of dye adsorption, the freshly prepared porous layers have been immersed in ethanol-based solution of red dye molecules at a concentration of 0.3 mM at

* Corresponding author. E-mail: duerr@sony.de Phone: ++49 711 5858418. Fax: ++49 711 5858484.

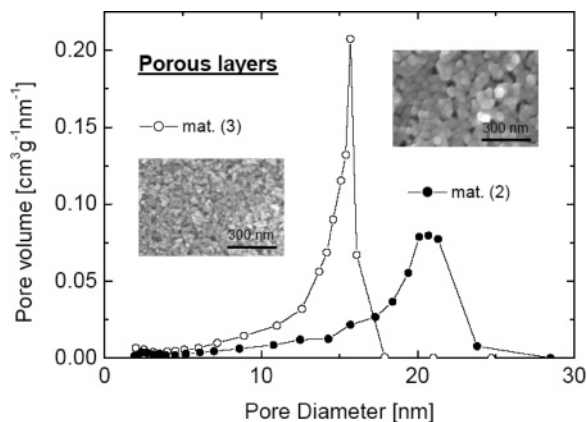


Figure 1. BJH analysis of the nitrogen desorption measurements as a measure of the pore openings in the porous films for two different materials. Material (3) shows in average smaller pore sizes but more pores of smaller size than material (2). Insets: scanning electron micrographs of the corresponding porous films.

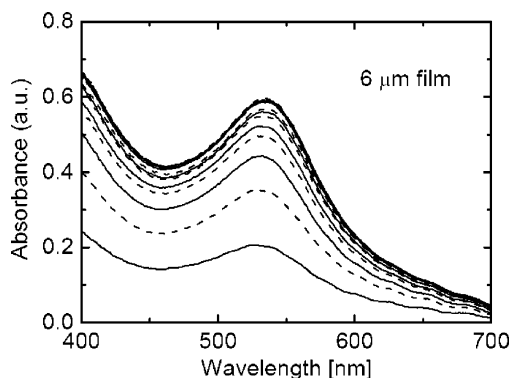


Figure 2. UV-vis spectra of a 6 μm thick TiO_2 film after subsequent coloring steps in 0.3 mM dye solution for 30 min each. The spectrum of a freshly prepared sample has been subtracted as baseline. The maximum in absorption corresponds to the absorption maximum of red dye.

room temperature (22 $^\circ\text{C}$). An influence of diffusion through the bulk solution or depletion of the dye in the solution on the adsorption experiments was prevented by mildly stirring the solution and by using a sufficient volume of dye solution, respectively. UV-vis spectra were taken of the fresh and colored films using that one of the fresh film for baseline correction. For the measurement of the partially colored films, the porous layers have been first rinsed in ethanol and dried with nitrogen. To minimize the influence of fluctuations in the thickness of each layer, much care has been taken to measure always at the same spot of the film. All the spectra taken show distinct absorption bands of red dye at about 530 nm. The height of the maximum of absorbance has been taken as a measure of the amount of dye molecules adsorbed on the TiO_2 surface and a linear dependence between these two values has been established by means of dye desorption in diluted NaOH ($c = 0.5 \text{ M}$).

Typical UV-vis absorption data are shown in Figure 2 for the adsorption of red dye on TiO_2 particles of a 6 μm thick film of material (1). A decrease in adsorption speed with increasing amount of adsorbed dye molecules as well as a later saturation can be easily observed from the spectra taken subsequently with constant time intervals. This is shown even clearer in Figure 3 where the absorbance in the maximum is plotted as a function of time for three layers of different thickness. For better comparison of the three layers, the

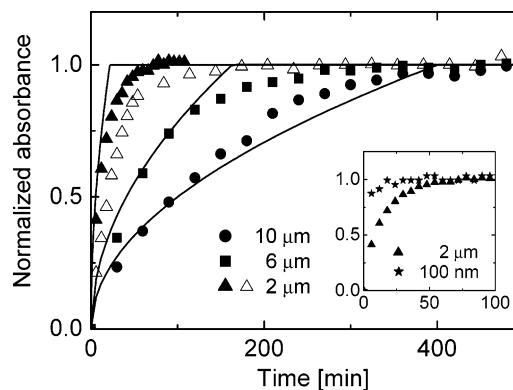


Figure 3. Normalized peak absorbance as a function of time for porous TiO_2 layers of different thickness (material (1), filled symbols). The solid lines represent fits of eq 2 to these data. Open triangles: results for a 2 μm thick TiO_2 film of material (3). Inset: comparison of data for 2 μm and 100 nm thick films.

absorbance values have been normalized to the saturation value of each layer, respectively. In such a representation, the curves are expected to lie on each other if the adsorption process itself is the rate-limiting step. In this case only the saturation level, but not the time dependence, should change. However, one clearly depicts different uptake curves indicating the influence of diffusion on the adsorption process. In fact, the initial part of the three curves in the nonnormalized representation (not shown) is nearly the same pointing toward a completely diffusion limited process. In the case of pure diffusion limitation, the nonnormalized curves are expected to be identical unless they reach their saturation value. This can be easily illustrated: If dye adsorption, and with this dye consumption, are much faster than dye transportation, all the dye molecules are adsorbed in a thin region between a sublayer of already dye-covered TiO_2 material and a sublayer comprising material still uncovered. Therefore, the thickness of the whole layer is irrelevant for the dyeing process and the initial speed of the process must be the same for all layers. On the basis of the assumption of adsorption being much faster than diffusion through the network, a simple model for the amount of dye adsorbed on the TiO_2 particles in the porous network and the concentration profile of dye has been established. The three main aspects of the model are (a) the thin region where adsorption takes place can be neglected in comparison to the layer thickness and (b) in the part of the porous layer between this region of adsorption and the bulk liquid, all TiO_2 is covered to the maximum coverage with dye molecules and no adsorption takes place in this region. Therefore a linear gradient in dye concentration between zero at the region of adsorption (the condition for a diffusion-limited process) and c_0 , the initial dye concentration, at the porous layer-liquid interface is established. The longer the colored part of the layer is, the smaller is the concentration gradient and therefore the mass transport of dye molecules to the region of adsorption resulting in a decrease of the apparent adsorption rate as observed in the experiment. (c) In the part of the porous layer between the region of adsorption and the substrate, all TiO_2 is uncovered and the dye concentration in the penetrating liquid is zero. The latter assumption is only true after the initial concentration in the porous layer has been adsorbed. However, because this concentration is low and the adsorption process fast, it does not influence the diffusion-limited adsorption process. The situation is illustrated in Figure 4 for the region of adsorption being about midway between porous layer-liquid interface and substrate. With θ_0 being the maximum amount of dye molecules adsorbed per volume of porous TiO_2 , at x_0 , the

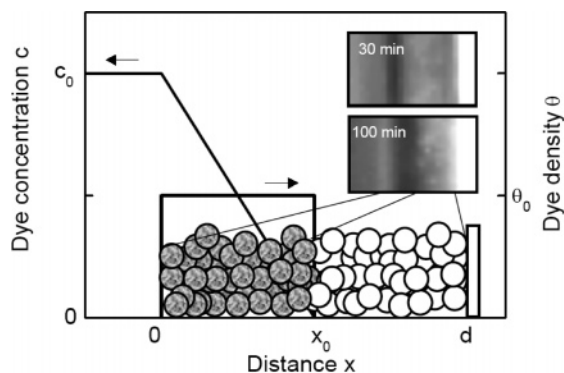


Figure 4. Representation of dye concentration in solution and dye coverage on the TiO₂ particles according to the suggested model. The dye concentration decreases linearly between c_0 at $x = 0$, the interface between porous layer and bulk solution, and zero at $x = x_0$, the region of adsorption. The amount of dye adsorbed is identical θ_0 in the region between $x = 0$ and $x = x_0$ and zero elsewhere. Inset: optical micrographs of cross sections of a 10 μm thick film after 30 and 100 min in dye solution. Bright at the right the glass substrate.

position of the region of adsorption, Fick's law can be written as

$$dt = \theta_0 / (Dc_0) x dx \quad (1)$$

Integration leads therefore to the following time dependence of x_0

$$\frac{x_0}{d} = \sqrt{\frac{2D_{\text{eff}}c_0}{\theta_0 d^2}} \cdot \sqrt{t} \quad (2)$$

when normalized to the layer thickness d . As the amount of dye adsorbed on the porous layer material is simply proportional to the position of the region of adsorption, x_0 , eq 2 reflects at the same time the time dependence of dye uptake for $x_0 < d$, i.e., for $t < t_{\text{max}} = \theta_0 d^2 / (2D_{\text{eff}}c_0)$, with t_{max} being the time it takes according to the model to fully color the porous layer. For $t > t_{\text{max}}$, the normalized position of the region of adsorption as well as the normalized amount of dye adsorbed stay constant and identical one. Knowing the average area taken by an adsorbed molecule to be 1.3 nm², the number of molecules adsorbed per volume, θ_0 , can be determined via the specific surface area and the porosity ϵ of the film and was calculated for red dye in the different layers under investigation to be between 8 and 12 $\times 10^{19}$ molecules/cm³. This allows a quantitative fitting of eq 2 to the data as shown in Figure 3. A good representation of the data of all films can be observed in the initial adsorption region up to 50% to 80% of the layer covered with dye molecules, and an effective diffusion constant of $D_{\text{eff}} = 7 \times 10^{-9}$ cm²/s can be derived for dye diffusion in material (1). To higher coverage and therefore longer adsorption time, the representation of the data by eq 2 is getting poorer, especially for the thin layers, pointing toward an oversimplification by the above applied model. However, diffusion seems still to be dominant because comparison between adsorption on a 2 μm and a 100 nm film prepared from similar particles as used in material (1) (Figure 3, inset) shows a pronounced difference and the adsorption rate for the 100 nm cannot be resolved within the time frame of our experiment. As a consequence of the agreement of the model with the data, one expects the porous layers to be fully colored in one part and uncolored in the other part of the film when it is taken out of the solution before the coloring process has been completed. As a rough check, approximately 10 μm thick samples similar to those described

above but with additional larger particles (300 nm in diameter, 20 w%) were prepared. These larger particles show increased light scattering and allow us to distinguish colored and uncolored parts of the layer when analyzed by means of optical microscopy. Cross sections of such films immersed in dye solution for limited times only are shown in the inset of Figure 4. Indeed, two different regions can be observed: e.g., after 100 min about 50% of the film is colored, in good agreement with the UV-vis data. To further check the applicability of the model, adsorption measurements with reduced dye concentrations have been performed. Qualitatively, they lead to the same adsorption curves; however, quantitatively they show a slower uptake in very good agreement to the $\sqrt{c_0}$ dependence in eq 2. Additionally, increased temperature accelerates the uptake of dye molecules, what is attributed to a temperature-activated increase of the effective diffusion constant.

For the investigation of the dependence of the diffusion constant on the properties of the porous material, layers with lower porosity but same particle size, material (2), as well as layers with comparable porosity but smaller particles, material (3), have been fabricated. Smaller particle size and lower porosity lead both to lower mean pore size. At comparable film thickness, the adsorption takes place much slower for the films with smaller pore size. As an example, the uptake curve for a 2 μm thick film of material (3) is included in Figure 3. From comparison of the initial part of the curves, a reduction of the effective diffusion constant in the finer porous layer, material (3), by a factor of 2 compared to material (1) can be determined. Diffusion in material (2), i.e., the same particles but lower porosity than (1), shows a similar behavior as (3). For better comparison, the values of the effective diffusion constants as well as for $D_0 = D_{\text{eff}}/\epsilon$ are given in Table 1.

For additional comparison, the diffusion constant for red dye in ethanol only has been determined by means of the porous frit method. The apparatus used, as well as the experimental procedure, are very similar to those described in ref 12. As a result, we obtained for bulk diffusion in ethanol $D_b = 4.2 \times 10^{-6}$ cm²/s, i.e., a value up to 3 orders of magnitude higher than found in the nanoporous TiO₂ network.

Besides porosity ϵ , diffusion in porous media is generally discussed in terms of tortuosity T and constrictivity δ . The tortuosity expresses the effective diffusion path through the porous media, which is longer than the layer thickness, and the constrictivity δ accounts for the fluctuations of the effective cross-sectional areas encountered in these diffusion paths. It holds $D_{\text{eff}} = \epsilon D_0 = \epsilon \delta / T^2 D_b = \epsilon / q_m D_b$ with the matrix factor q_m . Whereas the definition of tortuosity¹³ and its influence on diffusion is intuitive, the effect and measurement of the constrictivity seems to be more difficult. However, for various models applied, δ between 0.3 and 1 has been calculated.¹³ For the discussion of the high value of $q_m \approx 1000$ found in this investigation for the diffusion of dye molecules through nanoporous TiO₂, we therefore concentrate first on tortuosity. Diffusion measurements for tri-iodide in similar material have shown a matrix factor as low as 1.37.⁶ From this one can first conclude that, indeed, the constrictivity is small for the material under investigation because it is not expected to change dramatically with the size of the diffusing molecule. Second, the small value for q_m shows a strong dependence of q_m on molecule size as reported earlier⁹ and proves the existence of relatively straight diffusion channels through the porous network for smaller molecules. The reduction of the diffusibility for the dye molecules under investigation is therefore attributed to the fact that many of the pore connections are too small for the

diffusing molecules, resulting in a much longer effective diffusion length. The situation might be even enforced by the fact that the dye molecules have to diffuse through the porous TiO₂ with dye molecules already attached to the surface resulting in even smaller interconnections between the pores. However, this cannot be the only reason for the difference between I₃⁻ and dye diffusion because we have shown that the adsorbed dye has only a minor effect on the I₃⁻ diffusion properties.¹⁴ For diffusion in material (2) with reduced porosity, and with this also smaller size of pores and interconnections, the matrix factor further increases in accordance with the presented explanation. However, comparison of material (2) and material (3) shows only a small difference of the diffusion constant D_0 despite their pronounced difference in the size of particles, pores, and interconnections at same porosity. Nonetheless, this result, which is seemingly contradicting the above given explanation, can also be rationalized in the same framework. With in average smaller interconnections between the pores, the probability for the dye molecules to find interconnections too small for diffusion is increased. However, because the porosity is constant but the average pore size is reduced, the number of pores, and with this the number of interconnections between these pores, must be increased (compare also the BJH data shown in Figure 1). That means there exist more different possibilities for the dye molecules to diffuse through, and with this, the apparent diffusion length and matrix factor of (2) and (3) are similar. Of course, the interplay between molecule size, pore size, and particle size, and with this the distribution of pore sizes, is expected to play a decisive role and simulations of their influence on the diffusion process would be highly appreciated.

The values for matrix factors found in this investigation are also high when compared to values reported in the literature for the diffusion of molecules of different size in porous Vycor glass.^{8,9} Because Vycor shows in general a smaller pore size than the nanoporous TiO₂ of this investigation, the lower apparent tortuosity of Vycor may be explained by a more homogeneous distribution of the size of connections between the pores.⁸ To avoid misunderstandings, we would like to point out that this comparison of the size of interconnections between the pores does not necessarily enter the constrictivity, because the interconnections between pores that are too small for diffusion do not contribute to the diffusion paths and as a consequence not to the effective constrictivity.

In addition to the presented data, more detailed investigations on the influence of solvent and molecule–molecule interaction might be of interest. Experiments with porphyrin dyes have shown that strong interaction of the dye molecules leads to a very different adsorption/diffusion behavior.¹⁵ From the good applicability of our diffusion model, which neglects molecule–

molecule interaction, we observe only minor effects due to stacking or clustering of red dye molecules in the presented experiments.

As a result of the aforementioned extremely low diffusion constants, large-scale production processes of dye-sensitized solar cells reliant upon the simple staining of the porous layers from a bath of solution seem to be unpractical. Instead, techniques that assist the dye transport to the TiO₂ surface, e.g., by means of a turbulent flow of the dye solution through the porous layer,¹⁶ could be applied.

In summary, we have shown the adsorption of dye molecules on porous TiO₂ to be mostly diffusion limited. The diffusion constants vary with material properties but are found to be reduced by up to 3 orders of magnitude compared to diffusion in pure solvent. The correlated increase of the matrix factor is attributed to a strongly increased tortuosity because many smaller interconnections in the porous materials are not accessible for the larger dye molecules. The understanding of the influence and interplay of particle size, porosity, and pore size on the diffusion behavior may lead to a better control of the material properties on the nanometer scale. In addition, the detailed knowledge of the diffusion process enables an optimization of the coloring process in fabrication of dye-sensitized solar cells.

Acknowledgment. The authors would like to thank A. Bamedi, T. Miteva, and S. Rosselli for fruitful discussions and experimental help.

References and Notes

- (1) Fujishima, A.; Honda, K. *Nature* **1972**, *238*, 37.
- (2) Linsebigler, A. L.; Lu, G.; Yates, J. T. *Chem. Rev.* **1995**, *95*, 735.
- (3) Fujishima, A.; Rao, T. N.; Tryk, D. A. *J. Photochem. Photobiol.* **2000**, *C 1*, 1.
- (4) O'Regan, B.; Graetzel, M. *Nature* **1991**, *353*, 737.
- (5) Papageorgiou, N.; Barbe, C.; Grätzel, M. *J. Phys. Chem. B* **1998**, *102*, 4156.
- (6) Kron, G.; et al., *Electrochem. Sol. State Lett.* **2003**, *6*, E11.
- (7) Kärger, J.; et al., *J. Am. Ceram. Soc.* **1983**, *66*, 69.
- (8) Dozier, W. D.; Drake, J. M.; Klafter, J. *Phys. Rev. Lett.* **1986**, *56*, 197.
- (9) Guo, Y.; Langley, K. H.; Karasz, F. E. *Phys. Rev. B* **1994**, *50*, 3400.
- (10) Kainourgiakis, M. E.; Kikkikides, E. S.; Stubos, A. K.; Kanellopoulos, N. K. *J. Chem. Phys.* **1999**, *111*, 2735.
- (11) Barbé, C. B.; et al., *J. Am. Ceram. Soc.* **1997**, *80*, 3157.
- (12) Kostka, K. L.; Radcliffe, M. D.; von Meerwall, E. *J. Phys. Chem.* **1992**, *96*, 1189.
- (13) van Brakel, J.; Heertjes, P. M. *Int. J. Heat Mass Transf.* **1974**, *17*, 1093.
- (14) Dürr, M.; et al., *J. Chem. Phys.* **2004**, *121*, 11374.
- (15) Dürr, M.; Schmid, A.; Obermaier, M.; Yasuda, A.; Nelles, G. (in preparation).
- (16) Späth, M. et al., *Prog. Photovolt: Res. Appl.* **2003**, *11*, 207.